

Permanent magnet gearless traction drive for German high speed train *ICE 3*

A. Binder, Th. Koch
Department of Electrical Energy Conversion
Darmstadt University of Technology
D-64283 Germany

Abstract — Two different designs of permanent magnet motors as direct wheel-set drive for the German high speed train *ICE 3* are designed, one with surface mounted magnets (SM) and one with buried rotor magnets (BM). The surface magnet motor has 17 % less mass and a slightly higher efficiency and was therefore chosen for further investigations. Compared with the conventional drive system of the *ICE 3*, consisting of geared inverter fed induction machines, the gearless permanent magnet direct drive yields about 16 % lower losses. This calculation is based on the route parameters of the high speed track between Frankfurt/Main and Cologne in Germany, which is currently under construction.

I. INTRODUCTION

The German high speed train *ICE 3* (Fig. 1) operates up to 330 km/h and is driven by sixteen squirrel cage induction motors with a power of 500 kW per motor. Four motors are driven by one GTO-inverter as a group drive. The motors are distributed along the train, thus realizing a rail car concept with distributed driving power. The machines are open-circuit air-cooled.



Fig. 1: German high speed train *ICE 3*

The two high speed induction motors per bogie are operating via gear on the wheel-sets (Fig 2). Advantages of this system are small motor dimensions, cheap motor construction, good flux weakening performance and cost effective group operation.

In this paper, an alternative drive system is presented, consisting of gearless synchronous permanent magnet (PM) direct drive motors and a single drive IGBT-inverter configuration, where the motor is directly coupled to the wheel-set by flexible coupling in order to reduce the unsprung mass.

Motivation for this direct drive concept are the following advantages:

- Lower noise due to the missing gear
- Avoiding of oil maintenance
- No gear losses
- Reducing cost in maintenance
- No electric excitation
- Achieving a high efficiency
- Reduced energy consumption in train operation

Proceedings ICPE '01, Seoul

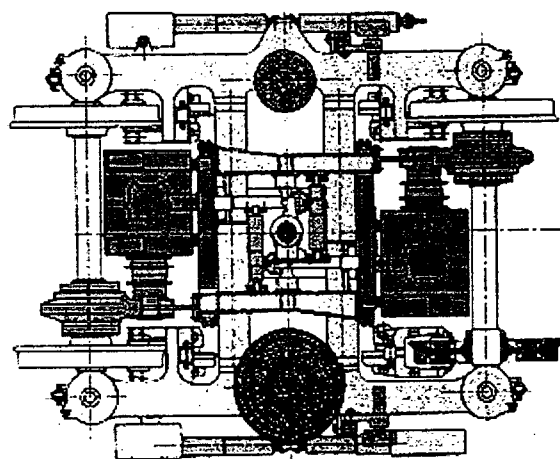


Fig. 2a: Actual bogie and the two induction motors of the *ICE 3*

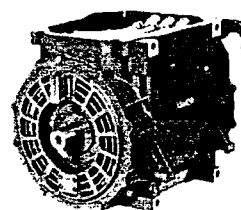


Fig. 2b: Actual squirrel cage induction motor of the *ICE 3*

A similar proposal has been already described in [2] and [5]. Alternatively, direct drive induction motors for electric traction have been designed and built some years ago. This solution is described in [6]. As direct drive electric machines must produce a big torque at low speed, a high pole count is advantageous. Therefore the PM synchronous machine seems to be the better solution than the induction motor, because a higher efficiency is possible.

II. DESIGN OF PM MOTORS

Design limits are the geometric and constructive conditions due to the maximum space given by the bogie as well as the maximum loads and restrictions given by the design for traction applications (Fig. 3).

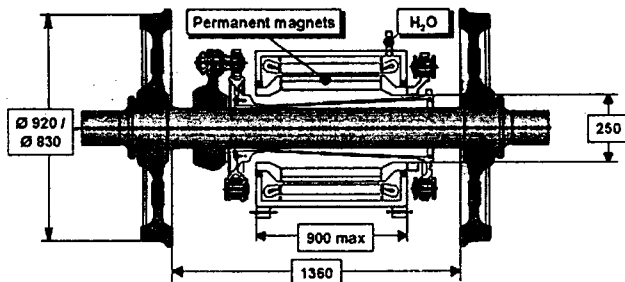


Fig. 3: Geometrical limits for PM motor design (dimensions in mm)

The electric restrictions are:

- The maximum phase voltage is given by the maximum voltage of the power converter, which is 810 V (rms).
- Limit of the product of current sheet A and current density J by about $A \cdot J \leq 7400 \text{ A/cm A/mm}^2$ is given by the used cooling system, a stator water jacket cooling.
- The height of the magnets and the pole pitch factor ($\alpha = 0.85$) are determined by the required flux to reach the demanded torque and to reduce space harmonics.
- Magnet height must be large enough to avoid irreversible demagnetization even under fault condition such as sudden short-circuit.
- Flux weakening must be possible via the stator current component I_d , so the synchronous reactance X_d must be large enough [3].

Table 1: Specifications of the PM motors for the high speed train ICE 3

Rated output P_N per motor	500 kW
Rated rotational speed n_N per wheel	617 / min
Maximum rotational speed n_{max} per wheel-set	2110 / min
Rated torque M_N per wheel-set	7700 Nm
Maximum torque M_{max} per wheel-set	8600 Nm
Maximum outer diameter d_{max} of the motor	590 mm
Maximum axial length of the motor	900 mm
Rated phase voltage U_N	810 V (rms)

Two different PM motor designs were calculated: Motor A has surface mounted magnets (SM) and long stator slots. Motor B has buried rotor magnets (BM) and short stator slots (Fig. 4 ÷ 5).

The design procedure for the motors consists of Finite Element (FEM) calculation for the flux quantities and analytical calculations for losses and stator voltage. Due to the high torque of 8.6 kNm and the rather low rated speed of 617/min a high pole count is advantageous and was chosen as $2p = 24$.

In Fig.6 and Fig.8 the flux patterns for rated torque are shown. The calculation was done with impressed stator current. The angle between the stator current phasor and the

rotor d-axis was varied, to get maximum torque. Calculation was done with the Finite Element program ANSYS.

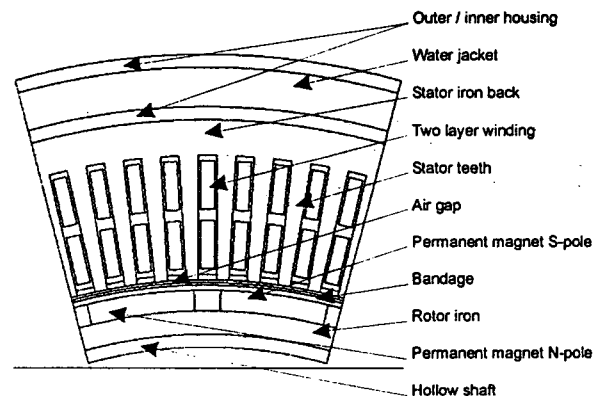


Fig. 4: Cross section of one pole pair of motor A

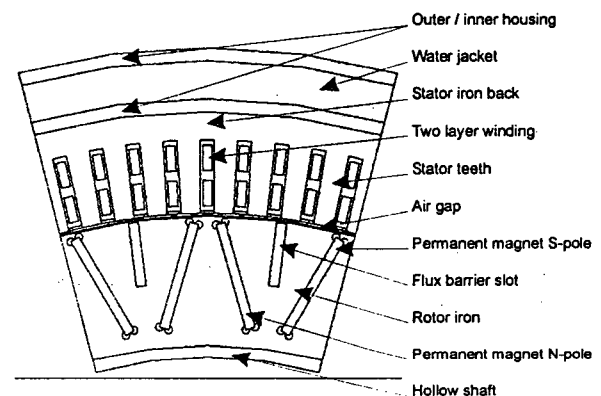


Fig. 5: Cross section of one pole pair of motor B

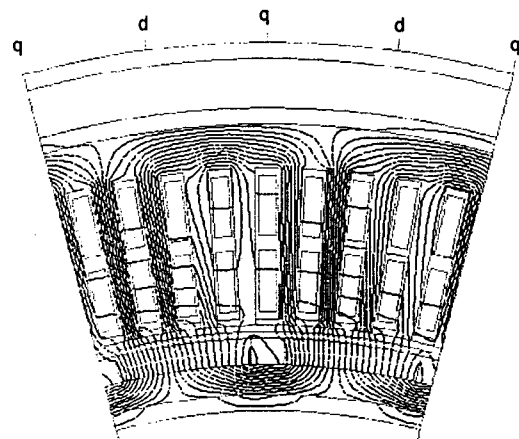


Fig. 6: Flux pattern of motor A (SM) at rated speed and power $P_N = 500 \text{ kW}$.

In order to calculate the required torque and to limit the terminal voltage simultaneously at its maximum value given by the power converter, an optimization procedure loop is used. With the help of the phasor diagram, the

terminal voltage is determined and is then compared with the maximum rated voltage. The optimization is finished when the voltage limit and the demanded torque are reached. All simulations are done with the above described two-dimensional FEM model of the motor using a static solution method.

The necessary d-component of the stator current to weaken the flux rises also with rising frequency and causes additional ohmic losses in the stator winding [3]. Motor A due to its better performance was chosen to be built as a prototype.

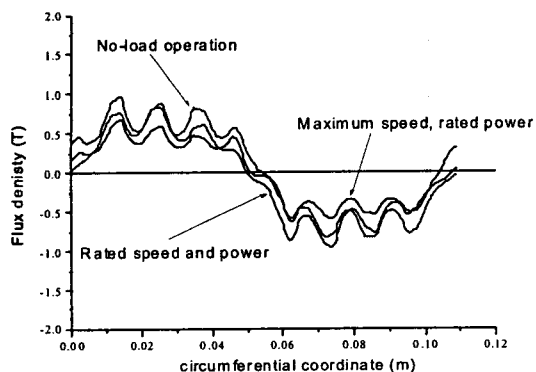


Fig. 7: Distribution of the radial component of the flux density in the middle of the air gap of motor A for three points of operation.

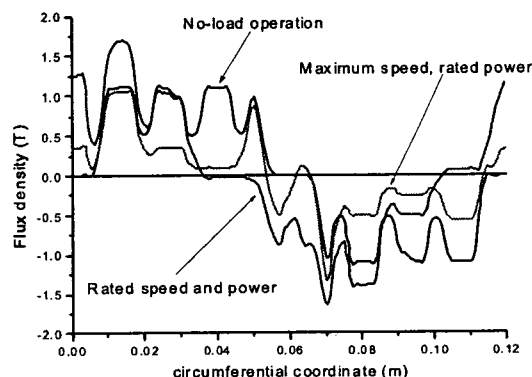


Fig. 9: Distribution of the radial component of the flux density in the middle of the air gap of motor B for three points of operation.

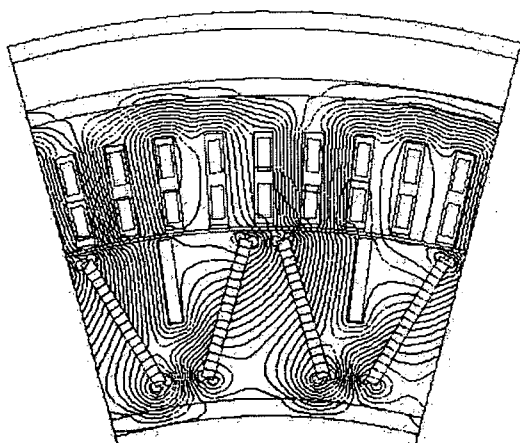


Fig. 8: Flux pattern of motor B (BM) at rated speed and power $P_N = 500$ kW.

As one result of calculations the total stator current consumption of motor A and B is compared. Motor B has a slightly higher rated current of 283 A than motor A with 251 A (Fig. 5).

Motor A has about 17 % less mass than motor B due to the thick and heavy rotor yoke of motor B. The total active masses are 466 kg for motor A. Flux weakening is achieved by a rotor position controlled field oriented control of the motors. The IGBT-inverter operates up to a rated frequency of 123.4 Hz in PWM mode, whereas in flux weakening range six-step operation is used.

Table 2 shows the slightly lower losses of motor A. For both motors the losses increase with rising frequency due to eddy-current losses in the copper winding and the iron parts.

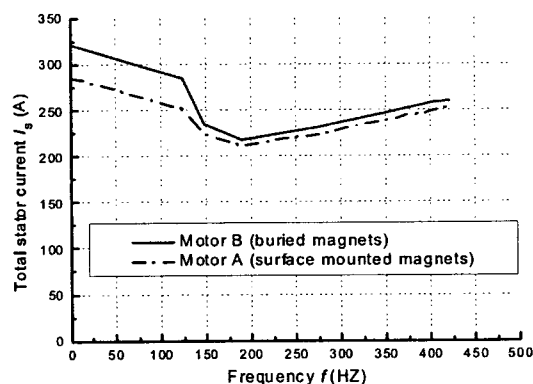


Fig. 10: Total stator current for motors A and B

Table 2: Calculated losses at sinusoidal supply at rated power:
a) 500 kW, 617 /min, 7700 Nm, 123.4 Hz,
b) 500 kW, 2110 /min, 2270 Nm, 422 Hz

Motor type	Motor A	Motor B
	a) / b)	a) / b)
Current I / A	251 / 253	283 / 260
Ohmic and conductor eddy current losses at 115 °C / W	14820 / 26864	15881 / 15818
Iron losses / W	5419 / 7755	6519 / 19223
Friction and windage losses / W	71 / 357	160 / 521
Eddy-current losses in the massive housing / W	251 / 61	465 / 410
Losses in the permanent magnets / W	20 / 101	- / -
Total losses P at sinusoidal supply / W	20581 / 35138	23025 / 35972

III. COMPARISON OF PM AND INDUCTION MOTOR

The chosen gearless PM motor A has a lower current consumption in the base speed range than the induction motor, but in the flux weakening range due to the necessary d-component of the stator current it exceeds the induction motor current significantly (Fig. 11).

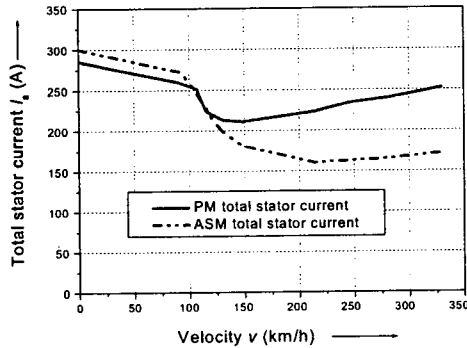


Fig. 11: Total stator current for PM motor A and the induction motor

A comparison of the PM direct drive concept and the geared induction motor concept concerning energy consumption was tried by evaluating the total energy consumption of the ICE 3 running on the planned route between Frankfurt/Main and Cologne. For this purposes the measured loss data of the inverter fed induction motor and of the gear were used. For the PM motor A the additional losses due to inverter supply were calculated analytically for different points of operations, given by torque and speed. In Table 3 these additional losses are shown for rated speed and maximum speed operation at rated power of 500 kW.

Table 3: Calculated losses of motor A with IGBT inverter operation at 500 kW output power

Operational speed	Rated	Maximum
Torque M / Nm	7700	2270
Speed n / 1/min	617	2110
Current I / A	251	253
Frequency f / Hz	123.4	422
Total losses P at sinusoidal supply	20581 W	35138 W
Inverter: Switching pattern	PWM $f_p=600$ Hz	Six-step
Iron losses due to inverter operation	61 W	43 W
Ohmic losses due to harmonic currents at 115 °C	256 W	15 W
Skin effect losses in copper conductors	475 W	505 W
Losses in the permanent magnets due to inverter operation	100 W	103 W
Total losses P_d	21 473 W	35 804 W

IV. ENERGY CONSUMPTION FOR THE ROUTE FRANKFURT/MAIN TO COLOGNE

The route between Frankfurt/Main and Cologne is 188 km long and has 18 bridges and 30 tunnels and is currently under construction. The route data of the slopes, of the acceleration and braking sections and of the stop time are given by the German Railway Company and were used to determine the demanded accelerating or braking motor torque. The given speed limits are used to calculate the necessary motor speed.

Table 4 and Table 5 show the demanded driving and braking data in connection with the corresponding travelling time for each operation point.

Table 4: Demanded driving data for the route between Frankfurt/Main and Cologne (speed n_i , torque M_i , time t_i , i -th operation point).

n_i	$M_i \times t_i$			
1/min	Nm x s			
105	8192 x 71	410 x 53		
316	8177 x 73	409 x 262		
527	7873 x 74	1181 x 119	394 x 16	
738	6518 x 88	1630 x 72	326 x 157	
949	5049 x 93	1767 x 39	265 x 12	
1160	4129 x 219	1032 x 105	619 x 72	
1371	3501 x 261	1225 x 68		
1582	3041 x 402			
1793	2682 x 478			
2004	2394 x 11	1796 x 13	1077 x 9	359 x 18

Table 5: Demanded braking data for the route between Frankfurt/Main and Cologne (speed n_i , torque M_i , time t_i , i -th operation point).

n_i	$M_i \times t_i$		
1/min	Nm x s		
105	8192 x 51		
316	8177 x 52		
527	7873 x 56		
738	6518 x 63	978 x 22	326 x 54
949	5049 x 60	253 x 21	
1160	4129 x 43		
1371	3501 x 51		
1582	3041 x 108		
1793	2682 x 69		
2004	2394 x 1	1317 x 29	

The total elapsed travelling time is 3914 s with 2770 s accelerating mode and 677 s in regenerative braking mode, whereas 467 s are consumed for train stop. The average train speed is 173 km/h. The calculated energy consumption of the PM gearless direct drive is 16.4 kWh for the whole distance, in comparison to the conventional gear induction motor with 19.5 kWh [4].

The new innovative traction drive concept consumes 3.1 kWh less than the asynchronous traction motor with gear, yielding a total energy saving of 49.6 kWh per train and 362 MWh per year (20 train journeys per day assumed).

The advantage of lower losses is only one positive aspect for a direct synchronous drive. Further advantages are lower noise, lower short circuit torque and avoiding of gear maintenance and oil leakage losses. Therefore the authors recommend this direct drive solution to be further investigated as a prototype for future high speed trains.

V. CONCLUSIONS

Two novel direct synchronous drives have been designed as a direct traction drive of the German high speed train *ICE 3* with the Finite Element method. These two types of motors were compared concerning mechanical data and performance. Motor A has a slightly lower total mass of about 640 kg, which is about 17 % less than that of motor B. Therefore, motor A is recommended to be built as a prototype. The calculated efficiency of this drive was compared with the existing geared asynchronous drive for the new high speed track from Frankfurt/Main to Cologne showing lower losses of about 16 %. This advantage – along with avoiding the gear and with lower torque ripple, lower short circuit torque and lower noise – might yield a powerful and innovative alternative to the existing geared asynchronous drive for the future.

VI. REFERENCES

- [1] Koch, Th.; Binder, A.: "Permanent magnet synchronous direct drive for high speed trains", *Proceedings of Electromotion '01*, Bologna 2001, pp. 287-292.
- [2] Kondou, K.; Matsuoka, K.: "Permanent Magnet Synchronous Motor Control System for Railway Vehicle Traction and its Advantages", *IEEE, PCC-Nagaoka*, 1997, pp. 63-68.
- [3] Binder, A.; Greubel, K.; Piepenbreier, B.; Tölle, H.-J.: "Permanent-Magnet Synchronous Drive with Wide Field-Weakening Range", *ETEP-Journal*, 8, 1998, pp. 157-166.
- [4] Koch, Th.; Binder, A.: "Energy saving with high speed trains propelled by direct permanent magnet synchronous drive", *Proceedings of the PCIM*, Nuremberg 2001.
- [5] Matsuoka, M.; Kondou, K.: "Conception of NEXT250 and Investigation of the Wheel-in Motor", *Proceedings of the National Conventional Record I.E.E.*, Japan Industry Application Society 1993, pp. 509-514.
- [6] Palik, F.; Kurbasow, A.: "Elektrischer Bahntrieb ohne Getriebe (Electrical traction drive without gear)", *Elektrische Bahnen 89(1991)*, pp. 66-70.
- [7] Leitgeb, W.: "Möglichkeiten des Direktantriebs oberer Hochleistungs-Fahrzeuge durch neue Wege der elektromechanischen Energiewandlung, Elektrische Triebfahrzeuge, *ZEVI + DET, Glas. Ann.* 119 (1995), No.9/10, pp. 408-413.
- [8] Binder, A.: Analytical calculation of eddy-current losses in massive rotor parts of high-speed permanent magnet machines, *Conference Proceedings of the Speedam 2000*, Ischia Italy, pp. C2/1-6.